J|A|C|S ARTICLES

Published on Web 09/10/2010

ortho-Phenylenes: Unusual Conjugated Oligomers with a Surprisingly Long Effective Conjugation Length

Jian He,[†] Jason L. Crase,[†] Shriya H. Wadumethrige,[‡] Khushabu Thakur,[‡] Lin Dai,[†] Shouzhong Zou,[†] Rajendra Rathore,[‡] and C. Scott Hartley*[,†]

Department of Chemistry and Biochemistry, Miami University, Oxford, Ohio 45056, and Department of Chemistry, Marquette University, P.O. Box 1881, Milwaukee, Wisconsin 53201

Received July 8, 2010; E-mail: scott.hartley@muohio.edu

Abstract: *ortho*-Phenylenes represent a fundamental but relatively unexplored class of conjugated molecular architecture. We have developed a robust synthetic approach to monodisperse *o*-phenylene oligomers which we have demonstrated by synthesizing a homologous series up to the dodecamer. The *o*-phenylenes exhibit complex conformational behavior but are biased toward a specific 2-fold-symmetric conformation which we believe corresponds to a stacked helix. Surprisingly, the series exhibits long-range delocalization, as measured by bathochromic shifts in UV/vis spectra. Although the overall magnitude of the shifts is modest (but comparable to some other classes of conjugated materials), the effective conjugation length of the series is approximately eight repeat units. The oligomers also exhibit an unusual hypsochromic shift in their fluorescence spectra with increasing length. The origin of these trends is discussed in the context of conformational analysis and DFT calculations of the frontier molecular orbitals for the series.

Introduction

Simple *ortho*-, *meta*-, and *para*-phenylene polymers constitute fundamental classes of conjugated structures and are the basic units of poly(phenylene)-based architectures now well established in organic electronics and nanotechnology.[1] In particular, the *p*-phenylenes have been extensively studied as active materials for organic electronics (e.g., as doped conducting polymers[2] and blue emitting materials for OLEDs[3]), as single molecule wires,[4] as scaffolds for the organization of other functionalities,[5] and in other applications. In contrast, the isomeric *o*-phenylenes have received very little attention. Like *p*-phenylenes, *o*-phenylenes are formally conjugated (in contrast to *m*-phenylenes, which are cross-conjugated[6]). However, the inherent twisting of the *o*-phenylene backbone limits orbital overlap in the π-system, and they are not expected to exhibit extensive through-bond conjugation. Accordingly, it has been reported that *o*-phenylenes do not exhibit significant π-electron delocalization, as measured by UV/vis spectroscopy.[1a,7]

A small number of *o*-phenylenes and related structures have been reported in the literature. As early as the 1960s, Kovacic reported that oxidative polymerization of toluene and chlorobenzene results in *o*-phenylene polymers.[8] However, the resulting materials are not structurally well-defined (e.g., believed to contain planar triphenylene-like structural defects), and polymers obtained by this method have not been extensively characterized. More recently, the electrochemical polymerization of catechol and its derivatives was reported to give poly(*o*-phenylene)s,[9] but these studies have subsequently been questioned and it is likely that only triphenylene-like molecules result from these reactions.[10]

The most direct parallels to the work reported in this paper are Ito's poly(2,3-quinoxaline)s[11] and Simpkins' synthesis of a genuine series of *o*-phenylene oligomers (up to the nonamer).[12] Both of these systems exhibit well-defined, but very different,

[†] Miami University.
[‡] Marquette University.

(1) (a) Berresheim, A. J.; Müller, M.; Müllen, K. *Chem. Rev.* **1999**, *99*, 1747–1785. (b) Grimsdale, A. C.; Müllen, K. *Macromol. Rapid Commun.* **2007**, *28*, 1676–1702. (c) Schmaltz, B.; Weil, T.; Müllen, K. *Adv. Mater.* **2009**, *21*, 1067–1078.
(2) Ivory, D. M.; Miller, G. G.; Sowa, J. M.; Shacklette, L. W.; Chance, R. R.; Baughman, R. H. *J. Chem. Phys.* **1979**, *71*, 1506–1507.
(3) (a) Grem, G.; Leditzky, G.; Ullrich, B.; Leising, G. *Adv. Mater.* **1992**, *4*, 36–37. (b) Kraft, A.; Grimsdale, A. C.; Holmes, A. B. *Angew. Chem., Int. Ed.* **1998**, *37*, 402–428. (c) Grimsdale, A. C.; Chan, K. L.; Martin, R. E.; Jokisz, P. G.; Holmes, A. B. *Chem. Rev.* **2009**, *109*, 897–1091.
(4) (a) Schlicke, B.; Belser, P.; De Cola, L.; Sabbioni, E.; Balzani, V. *J. Am. Chem. Soc.* **1999**, *121*, 4207–4214. (b) Weiss, E. A.; Ahrens, M. J.; Sinks, L. E.; Gusev, A. V.; Ratner, M. A.; Wasielewski, M. R. *J. Am. Chem. Soc.* **2004**, *126*, 5577–5584. (c) Holman, M. W.; Liu, R.; Zang, L.; Yan, P.; DiBenedetto, S. A.; Bowers, R. D.; Adams, D. M. *J. Am. Chem. Soc.* **2004**, *126*, 16126–16133. (d) Banerjee, M.; Shukla, R.; Rathore, R. *J. Am. Chem. Soc.* **2009**, *131*, 1780–1786.
(5) (a) Sakai, N.; Mareda, J.; Matile, S. *Acc. Chem. Res.* **2005**, *38*, 79–87. (b) Bhosale, S.; Sisson, A. L.; Talukdar, P.; Fürstenberg, A.; Banerji, N.; Vauthey, E.; Bollot, G.; Mareda, J.; Röger, C.; Würthner, F.; Sakai, N.; Matile, S. *Science* **2006**, *313*, 84–86. (c) Sisson, A. L.; Sakai, N.; Banerji, N.; Fürstenberg, A.; Vauthey, E.; Matile, S. *Angew. Chem., Int. Ed.* **2008**, *47*, 3727–3729.
(6) Hong, S. Y.; Kim, D. Y.; Kim, C. Y.; Hoffmann, R. *Macromolecules* **2001**, *34*, 6474–6481.
(7) (a) Noren, G. K.; Stille, J. K. *Macromol. Rev.* **1971**, *5*, 385–430. (b) Tour, J. M. *Adv. Mater.* **1994**, *6*, 190–198.
(8) (a) Kovacic, P.; Uchic, J. T.; Hsu, L.-C. *J. Polym. Sci., Part A: Polym. Chem.* **1967**, *5*, 945–964. (b) Kovacic, P.; Ramsey, J. S. *J. Polym. Sci., Part A: Polym. Chem.* **1969**, *7*, 111–125. (c) Hsing, C.-F.; Jones, M. B.; Kovacic, P. *J. Polym. Sci., Part A: Polym. Chem.* **1981**, *19*, 973–984.
(9) (a) Xu, J.; Liu, H.; Pu, S.; Li, F.; Luo, M. *Macromolecules* **2006**, *39*, 5611–5616. (b) Dong, B.; Zheng, L.; Xu, J.; Liu, H.; Pu, S. *Polymer* **2007**, *48*, 5548–5555. (c) Ma, M.; Liu, H.; Xu, J.; Li, Y.; Wan, Y. *J. Phys. Chem. C* **2007**, *111*, 6889–6896.
(10) Voisin, E.; Williams, V. E. *Macromolecules* **2008**, *41*, 2994–2997.

10.1021/ja106050s

secondary structures: unlike the rod-like *p*-phenylenes, *o*-phenylenes have the potential for a rich conformational behavior, as the backbone can assume a variety of distinct conformational states due to hindered rotation and torsional biases about the biaryl bonds. In principle, this could lead to intractable mixtures of random, slowly interconverting conformers. However, extensive studies of the poly(2,3-quinoxaline)s have established that they adopt an extended helical conformation both in solution and in the solid state.[11] The *o*-phenylenes themselves have received much less attention, but Simpkins' study does include a crystal structure of an *o*-phenylene hexamer that establishes a compact helical conformation.[12]

Even if *o*-phenylenes do not exhibit extensive through-bond delocalization, we reasoned that they still have considerable potential as functional organic nanostructures (e.g., in terms of charge or energy transport). For example, Müllen-type polyphenylene dendrimers have been used to spatially organize chromophores for efficient energy transport,[13] and interarene electronic interactions within the dendritic arms have been demonstrated despite high bond torsions.[14] Porous polyphenylene frameworks have also recently been shown to undergo efficient energy transfer.[15] Further, DNA has attracted considerable attention as a charge-transport medium,[16] even though the UV/vis spectrum of an extended DNA polymer is essentially a superposition of the spectra of the constituent bases,[17] implying limited ground-state conjugation. It is the spatial organization of the chromophores that makes these materials interesting. Analogously, the *o*-phenylene architecture may provide a convenient means to organize chromophores into dense arrays. If the secondary structure of *o*-phenylenes is well-defined and can be established and controlled, then they may exhibit interesting through-space interactions between aromatic monomers. Ultimately, we believe these systems may be relevant as novel approaches to molecular wires and also as models for transport phenomena in DNA, organic thin films, and π-stacked columnar aggregates.

Nevertheless, very few well-characterized examples of *o*-phenylenes have been synthesized, and very little is known of their conformational behavior and electronic structure. Here we present a robust synthetic approach to monodisperse *o*-phenylene oligomers, which we have demonstrated by synthesizing the homologous series **oP^n** up to the dodecamer. This is significantly longer than previously reported *o*-phenylenes, which has allowed us to observe systematic changes in electronic properties as a function of the number of arene repeat units (*n*). We have found that the **oP^n** series exhibits several very unusual properties compared to typical conjugated architectures, including a surprisingly long effective conjugation length as measured by UV/vis spectroscopy and a hypsochromic shift in fluorescence spectra with increasing length. These results are discussed in the context of the secondary structure of the oligomers and ab initio calculations of their frontier molecular orbitals.

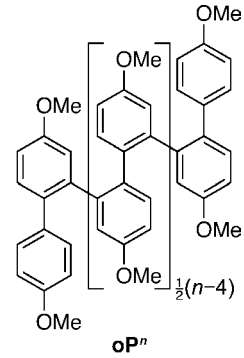

oP^n

Results

Synthesis. In general, the synthesis of monodisperse oligomers requires bifunctional monomers in which the reactivity of at least one reactive group can be controlled.[18] In Simpkins' original synthesis of *o*-phenylenes, this was accomplished by taking advantage of the greater reactivity of aryl iodides, compared to aryl bromides, toward Suzuki−Miyaura coupling; however, only low yields were obtained for the higher oligomers.[12] For our series, we wished to apply recent developments in iterative oligo(phenylene) synthesis via Suzuki−Miyaura coupling.[19] In our hands, methods[19a,b] based on the deactivation of the boronic acid were unsuccessful in the synthesis of **oP^n**, due to undesired side reactions or difficulties in purifying and characterizing the resulting sterically hindered products. However, Manabe's approach based on the use of phenols as masked triflates, which they had demonstrated with the synthesis of an *o*-phenylene pentamer,[19c] was readily applied to the synthesis of the **oP^n** series.

We based our synthesis on 9,10-boroxarophenanthrene derivative **1**, as it allowed two arene units to be added in a single step, and because the desired substitution pattern was readily installed. Similar boroxarenes have previously been shown to undergo Suzuki−Miyaura coupling.[20] Traditionally, these compounds have been prepared by treatment of the appropriate 2-hydroxybiphenyl with BCl_3;[21] however, we found it convenient to prepare monomer **1** from readily available 2,2′-dibromo-5,5′-dimethoxybiphenyl[22] via a series of metal−halogen exchanges, as shown in Scheme 1.

With monomer **1** in hand, the synthesis of the **oP^n** series was carried out according to Scheme 2. Suzuki−Miyaura coupling of **1** with 4-iodoanisole using Buchwald's SPhos catalyst[23] gave trimer **oP^3-OH**, which was then activated toward further

(11) (a) Ito, Y.; Ihara, E.; Murakami, M. *J. Am. Chem. Soc.* **1990**, *112*, 6446–6447. (b) Ito, Y.; Ihara, E.; Murakami, M. *Angew. Chem., Int. Ed. Engl.* **1992**, *31*, 1509–1510. (c) Ito, Y.; Miyake, T.; Hatano, S.; Shima, R.; Ohara, T.; Suginome, M. *J. Am. Chem. Soc.* **1998**, *120*, 11880–11893. (d) Ito, Y.; Ohara, T.; Shima, R.; Suginome, M. *J. Am. Chem. Soc.* **1996**, *118*, 9188–9189. (e) Suginome, M.; Collet, S.; Ito, Y. *Org. Lett.* **2002**, *4*, 351–354.
(12) Blake, A. J.; Cooke, P. A.; Doyle, K. J.; Gair, S.; Simpkins, N. S. *Tetrahedron Lett.* **1998**, *39*, 9093–9096.
(13) (a) Weil, T.; Reuther, E.; Müllen, K. *Angew. Chem., Int. Ed.* **2002**, *41*, 1900–1904. (b) Bauer, R. E.; Grimsdale, A. C.; Müllen, K. *Top. Curr. Chem.* **2005**, *245*, 253–286.
(14) Liu, D. J.; De Feyter, S.; Cotlet, M.; Stefan, A.; Wiesler, U.-M.; Herrmann, A.; Grebel-Koehler, D.; Qu, J.; Müllen, K.; De Schryver, F. C. *Macromolecules* **2003**, *36*, 5918–5925.
(15) Chen, L.; Honsho, Y.; Seki, S.; Jiang, D. *J. Am. Chem. Soc.* **2010**, *132*, 6742–6748.
(16) Porath, D.; Cuniberti, G.; Di Felice, R. *Top. Curr. Chem.* **2004**, *237*, 183–227.
(17) Eisinger, J.; Shulman, R. G. *Science* **1968**, *161*, 1311–1319.
(18) Franz, N.; Kreutzer, G.; Klok, H.-A. *Synlett* **2006**, 1793–1815.
(19) (a) Noguchi, H.; Hojo, K.; Suginome, M. *J. Am. Chem. Soc.* **2007**, *129*, 758–759. (b) Gillis, E. P.; Burke, M. D. *J. Am. Chem. Soc.* **2007**, *129*, 6716–6717. (c) Ishikawa, S.; Manabe, K. *Chem. Lett.* **2006**, *35*, 164–165.
(20) Zhou, Q. J.; Worm, K.; Dolle, R. E. *J. Org. Chem.* **2004**, *69*, 5147–5149.
(21) (a) Dewar, M.; Dietz, R. *J. Chem. Soc.* **1960**, 1344–1347. (b) Greig, L. M.; Kariuki, B. M.; Habershon, S.; Spencer, N.; Johnston, R. L.; Harris, K. D. M.; Philp, D. *New J. Chem.* **2002**, *26*, 701–710.
(22) Campbell, N.; Scott, A. H. *J. Chem. Soc. C* **1966**, 1050–1052.
(23) Walker, S. D.; Barder, T. E.; Martinelli, J. R.; Buchwald, S. L. *Angew. Chem., Int. Ed.* **2004**, *43*, 1871–1876.

Scheme 1. Synthesis of Monomer **1**[a]

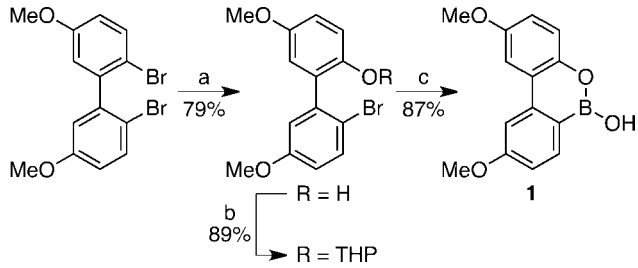

[a] Reagents and conditions: (a) (i) ^{n}BuLi, THF, −78 °C, 1 h; (ii) B(O^{i}Pr)$_3$, 12 h; (iii) NaOH, H_2O_2, H_2O, 5 h; (b) dihydropyran, PPTS, CH_2Cl_2, overnight; (c) (i) ^{n}BuLi, THF, −78 °C; (ii) B(O^{i}Pr)$_3$, 12 h; (iii) HCl(aq), 1.5 h.

coupling by triflation (to give **oP^3-OTf**). The oligomer could be extended to **oP^5-OH** at this point by coupling with another equivalent of **1** or capped by coupling with 4-methoxyphenylboronic acid to give **oP^4** (alternatively, **oP^4** can be prepared directly by coupling of 2,2′-dibromo-5,5′-dimethoxybiphenyl with 4-methoxyphenylboronic acid). Repetition of this sequence allowed the higher oligomers **oP^6**−**oP^{12}** to be prepared. This method affords consistently good yields at each step and should be readily extended beyond the dodecamer. Using this approach, we were able to prepare >300 mg of each member of the series in a single synthetic effort.

In contrast to *p*-phenylenes, all compounds in Scheme 2 exhibit excellent solubility in organic solvents despite lacking explicit solubilizing groups, as is expected for *o*-phenylenes.[1a,7b] NMR spectra of the longer oligomers, beginning with **oP^5-OH**, are complicated by slow conformational exchange on the NMR time scale, which is unsurprising given the steric hindrance of the *o*-phenylene backbone. Thus, while **oP^4** exhibits a readily interpreted first-order ^{1}H NMR spectrum (Figure S1), the spectrum of **oP^6** consists of broad signals at room temperature (Figure S2), although sharp, well-resolved signals are obtained by cooling to −5 °C. The major signals in this spectrum can be fully assigned to the proposed structure, including its 2-fold symmetry, although small unassigned signals remain. The higher oligomers **oP^8**−**oP^{12}** give relatively sharp ^{1}H NMR spectra at room temperature (Figures S3−S5); again, the major signals in the spectra can be fully assigned to the expected structures, but there are additional minor signals. We believe that the small signals in the NMR spectra result not from impurities but from less-significant conformational states in slow exchange on the NMR time scale. This is supported by the observation that all ^{1}H NMR signals for each oligomer broaden and coalesce at elevated temperature (spectra at 100 °C in DMSO-d_6 are included in the Supporting Information). In another report, a related *o*-phenylene hexamer required elevated temperatures for NMR characterization.[24] Unfortunately, we were unable to reach a fast exchange regime for our oligomers within the limitations of our instrumentation (150 °C).

All isolated **oP^n** exhibit exceptionally clean MALDI mass spectra (Figure 1), which are qualitatively consistent with high purity given that all other synthetic intermediates also give strong MALDI signals under the same conditions. The elemental composition of the oligomers is confirmed by the excellent match between the experimental and theoretical isotopic distributions of the MALDI peaks. Gel permeation chromatography of **oP^6**−**oP^{12}** also indicated high purity, with single monomodal peaks for each oligomer (Figure S6; **oP^4** elutes too close to the permeation limit of our column). The oligomers were also characterized by elemental analysis.

Crystals of **oP^4** and **oP^6** were grown by crystallization from CH_2Cl_2/MeOH and CH_2Cl_2/MeCN, respectively, and their structures were determined by X-ray crystallography, as shown in Figure 2. The overall backbone conformation of an **oP^n** oligomer is defined by the dihedral angles of its biaryl bonds (ϕ_i, where *i* indexes the bonds starting at one end; see Figure 2 for examples). In the solid state, **oP^4** adopts a quasi-C_2-symmetric helical conformation with backbone bond torsions of $\phi_1 = 42.4°$, $\phi_2 = 55.6°$, and $\phi_3 = 44.9°$. The outermost rings are offset stacked, with 4.16 Å between their centers and a very close contact of 3.15 Å between C14 and C44. This structure is similar to that of another recently reported *o*-quaterphenyl.[25] Conversely, the solid-state structure of **oP^6** is not purely helical. The backbone again assumes a quasi-C_2-symmetric conformation ($\phi_1 = 127.4°$, $\phi_2 = 135.2°$, $\phi_3 = -74.4°$, $\phi_4 = 138.0°$, $\phi_5 = 131.4°$), although the orientations of the terminal methoxy groups break the overall symmetry of the molecule. The four central arenes in **oP^6** are arranged as a stacked helix analogous to the conformation of **oP^4**; however, the outermost rings are flipped away from the helical path. Interestingly, this contrasts with the π-stacked, entirely helical conformation observed by Simpkins and co-workers for their *o*-phenylene hexamer.[12]

UV/vis Spectroscopy. UV/vis spectra of **oP^2**−**oP^{12}** in dichloromethane are given in Figure 3 (**oP^2** = 4,4′-dimethoxybiphenyl). In general, the spectra are broad and featureless, with little qualitative change in shape for $n \geq 4$. The oligomers exhibit no significant UV/vis solvatochromism, as indicated by comparison with spectra of methanol and hexanes solutions (Figure S7). There is also very little difference between the solution and solid-state spectra of **oP^{12}** (compare Figures 3 and S8). Normalization of the spectra with respect to *n* (Figure S9) reveals a substantial hypochromic effect; i.e., the intensities of the bands centered around 270 nm decrease substantially with oligomer length, with a corresponding increase in the intensities at both longer (>300 nm) and shorter (<250 nm) wavelengths. This effect is largest for **oP^{12}**, which has a hypochromicity of approximately 60% at 270 nm vs **oP^2**. This behavior is highly reminiscent of DNA, where it arises from the parallel stacking of the transition dipole moments of the bases.[26] Hypochromicity has also been observed in other π-stacked systems.[27] In the present case, analysis of this effect is complicated as the individual monomers likely cannot be treated as independent chromophores. However, it is noteworthy that for arenes it is generally assigned to parallel stacked geometries, which is consistent with the conformational analysis discussed below.[28]

(24) Ormsby, J. L.; Black, T. D.; Hilton, C. L.; Bharat; King, B. T. *Tetrahedron* **2008**, *64*, 11370–11378.

(25) Nehls, B. S.; Galbrecht, F.; Bilge, A.; Brauer, D. J.; Lehmann, C. W.; Scherf, U.; Farrel, T. *Org. Biomol. Chem.* **2005**, *3*, 3213–3219.

(26) (a) Bloomfield, V. A.; Crothers, D. M.; Tinoco, I., Jr. *Physical Chemistry of Nucleic Acids*; Harper & Row: New York, 1974. (b) Tinoco, I., Jr. *J. Am. Chem. Soc.* **1960**, *82*, 4785–4790.

(27) (a) Lokey, R. S.; Iverson, B. L. *Nature* **1995**, *375*, 303–305. (b) Nelson, J. C.; Saven, J. G.; Moore, J. S.; Wolynes, P. G. *Science* **1997**, *277*, 1793–1796. (c) Nakano, T.; Yade, T. *J. Am. Chem. Soc.* **2003**, *125*, 15474–15484. (d) Goto, H.; Katagiri, H.; Furusho, Y.; Yashima, E. *J. Am. Chem. Soc.* **2006**, *128*, 7176–7178. (e) Sinkeldam, R. W.; Hoeben, F. J. M.; Pouderoijen, M. J.; De Cat, I.; Zhang, J.; Furukawa, S.; De Feyter, S.; Vekemans, J. A. J. M.; Meijer, E. W. *J. Am. Chem. Soc.* **2006**, *128*, 16113–16121.

(28) Cantor, C. R.; Schimmel, P. R. *Biophysical Chemistry*; W. H. Freeman and Company: San Francisco, 1980.

Scheme 2. Iterative Synthesis of **oP^n** Oligomers[a]

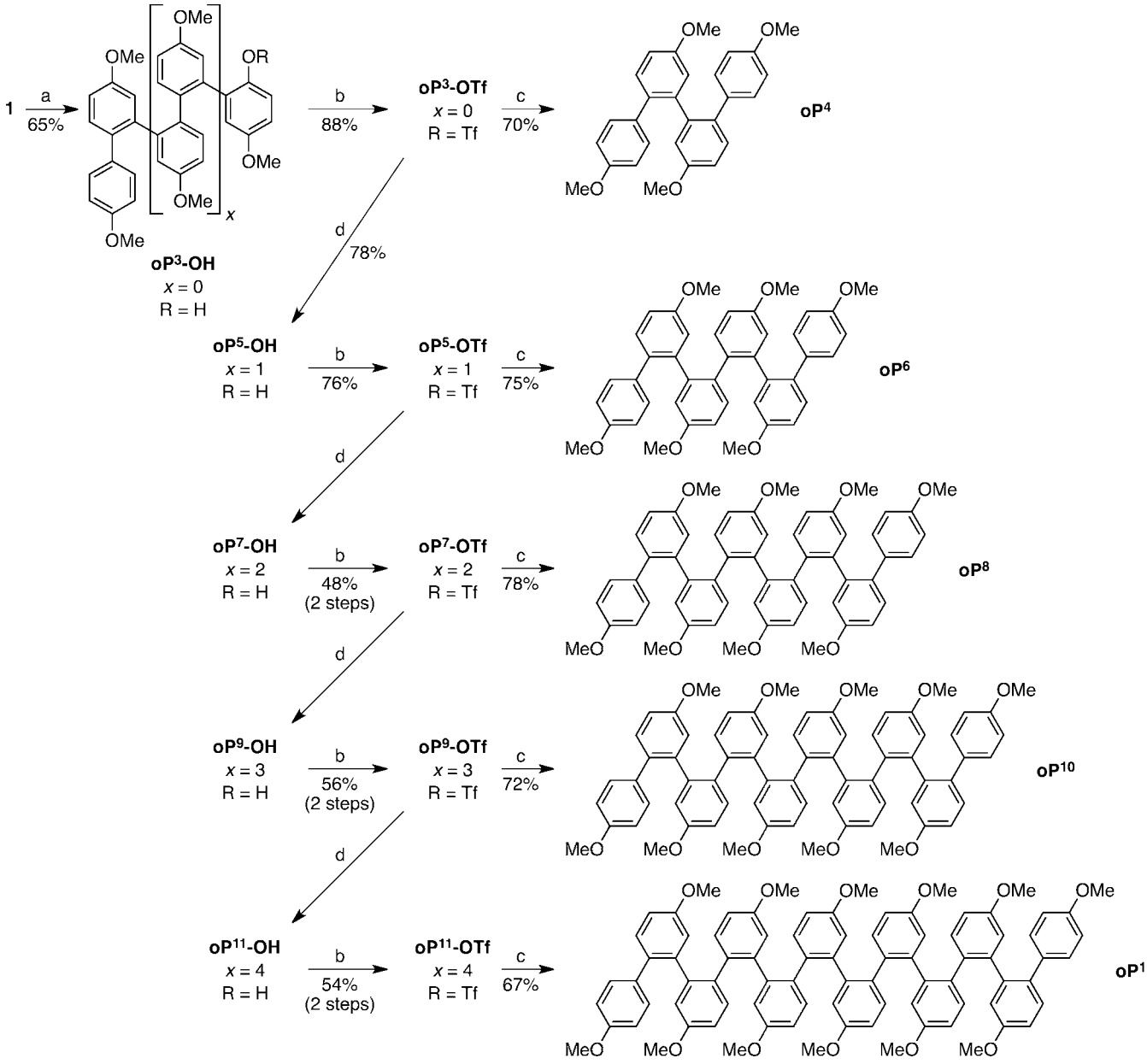

[a] Reagents and conditions: (a) 4-iodoanisole, $Pd(OAc)_2$, SPhos, K_3PO_4, THF, 90 °C, overnight; (b) Tf_2O, pyridine, CH_2Cl_2, overnight; (c) 4-methoxyphenylboronic acid, $Pd(OAc)_2$, SPhos, K_3PO_4, THF/H_2O (4:1), 100 °C, overnight; (d) **1**, $Pd(OAc)_2$, SPhos, K_3PO_4, THF/H_2O (4:1), 90 °C, overnight.

The evolution of electronic spectra as a function of oligomer length has long been established as a means to probe the extent of conjugative effects.[29] The degree of conjugation in conjugated oligomers is often evaluated by plotting observed UV/vis transition energies vs 1/*n*, which generally gives a good linear fit for relatively short oligomers (i.e., away from the asymptotic polymer limit as $n \rightarrow \infty$). To account for the observed deviations from linearity as *n* increases, Meier has developed an empirical method for the quantification of the extent of conjugation in conjugated oligomeric/polymeric systems based on a fit to eq 1:

$$\lambda_n = \lambda_\infty - \Delta\lambda \cdot e^{-b(n-1)} \qquad (1)$$

where λ_n is the wavelength of the relevant transition for an oligomer with *n* monomer units. The parameter λ_∞ is the extrapolation of λ_n to the polymer limit, and the parameters $\Delta\lambda = \lambda_\infty - \lambda_1$ and *b* quantify the overall effect of conjugation and the extent of conjugation, respectively, allowing comparisons to be made between different conjugated systems. From these parameters, it is possible to calculate the effective conjugation length of the system (n_{ecl}), which represents the number of monomer units over which there is significant delocalization. By definition, the effective conjugation length is the value of *n* for which the difference between λ_∞ and λ_n is less than 1 nm, which gives

$$n_{ecl} = \frac{\ln \Delta\lambda}{b} + 1 \qquad (2)$$

The UV/vis spectra of the **oP^n** series undergo a clear red shift from **oP^2** to **oP^6**; however, the absence of distinct maxima beyond $n = 4$ makes quantitative evaluation of the change in λ_{max} values, as is common for conjugated oligomers, impossible.

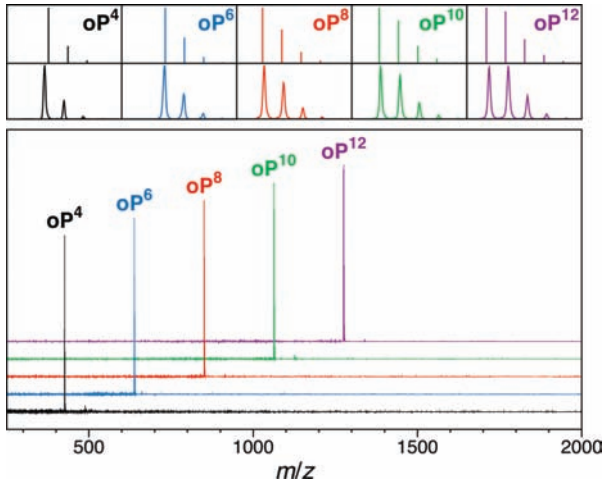

Figure 1. MALDI mass spectra of **oP^n** (dithranol matrix). Bottom: full experimental spectra. Top: experimental (bottom) and theoretical (top) isotopic distributions for each M^+ peak. **oP^4**: calcd 426.18, found 425.96; **oP^6**: calcd 638.27, found 638.22; **oP^8**: calcd 850.35, found 850.42; **oP^{10}**: calcd 1062.43, found 1062.50; **oP^{12}**: calcd 1274.52, found 1274.66.

Instead, we have evaluated onset absorption values ($\lambda_{ext,UV}$) obtained by extrapolation of the first turning point in the spectra to $\varepsilon = 0$ (Figure S10).[30] Similar results are obtained if the absorption onset is estimated as the point at which the ε values pass beyond a low threshold. In his original paper, Meier showed that similar data provide an equivalent measure of both the magnitude ($\Delta\lambda$) and degree (b) of conjugation for other systems.[31] Further, analysis of the data for the structurally related *p*-phenylenes[4d] indicates that the parameters ($\Delta\lambda_{UV}$, b_{UV}) are insensitive to the use of extrapolated onset data vs the more conventional peak maxima, confirming that $\lambda_{ext,UV}$ should provide useful parameters for the **oP^n** series that are appropriate for semiquantitative comparisons with other systems.

As shown in Figure 4, the obtained $\lambda_{ext,UV}$ values show very good fits to eq 1 and also show a clear linear dependence on $1/n$, implying that significant changes in the spectra are observed even up to $n = 12$. Fitting to eq 1, we extract values of $\lambda_{\infty,UV} = 325.5 \pm 0.5$ nm, $\Delta\lambda_{UV} = 39 \pm 2$ nm, and $b_{UV} = 0.52 \pm 0.05$. For the **oP^n** system, we estimate therefore that $n_{ecl} \approx 8$, based on eq 2.

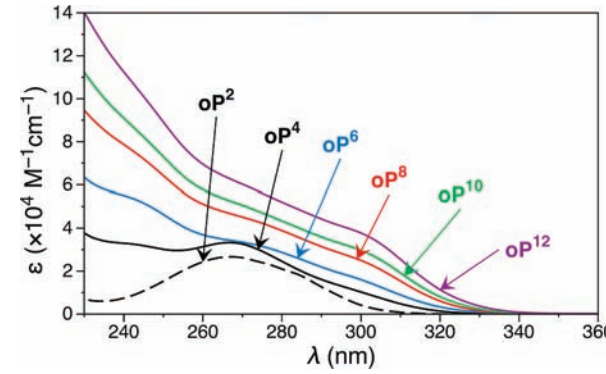

Figure 3. UV/vis spectra of **oP^2**−**oP^{12}** in dichloromethane.

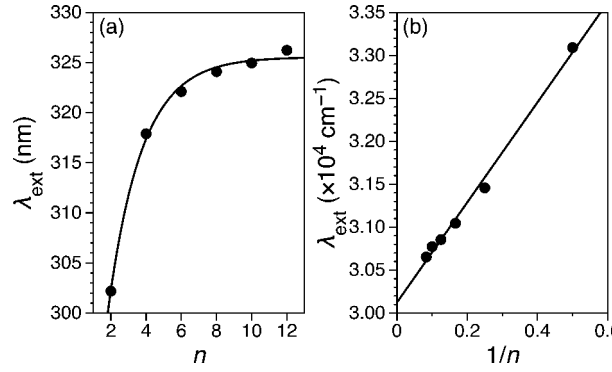

Figure 4. (a) Plot of $\lambda_{ext,UV}$ vs n; the solid line represents a fit to eq 1 ($\chi^2 = 1.50$). (b) Plot of $\lambda_{ext,UV}$ vs $1/n$; the solid line is a linear least-squares fit ($R^2 = 0.994$).

Fluorescence Spectroscopy. Fluorescence spectra for the **oP^n** series are shown in Figure 5. Overall, the oligomers are moderately fluorescent. Quantum yields were determined relative to DPA ($\Phi = 0.90$) following the established procedure.[32] The quantum yield for **oP^4** is comparatively low ($\Phi = 0.040$), but for the remaining oligomers it is moderate and relatively consistent (**oP^6**: $\Phi = 0.12$; **oP^8**: $\Phi = 0.19$; **oP^{10}**: $\Phi = 0.19$;

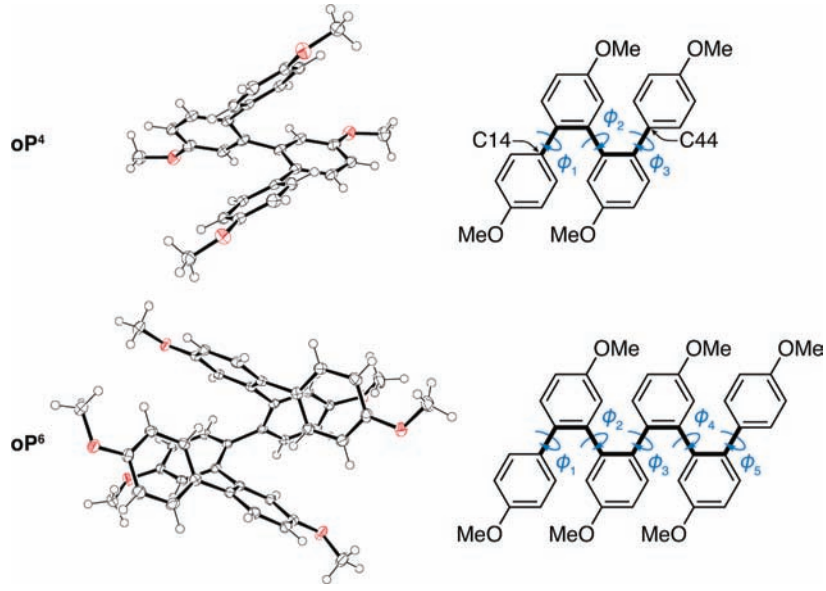

Figure 2. ORTEP representations (50% ellipsoid probability) of the crystal structures of **oP^4** and **oP^6**. A molecule of acetonitrile has been removed from the structure of **oP^6** for clarity.

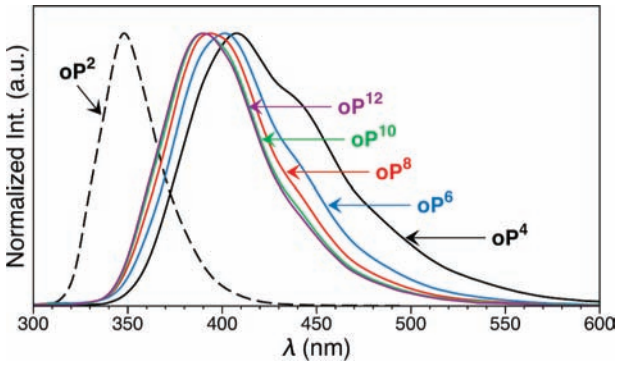

Figure 5. Normalized fluorescence spectra of **oP^n** in dichloromethane (excitation at 260 nm).

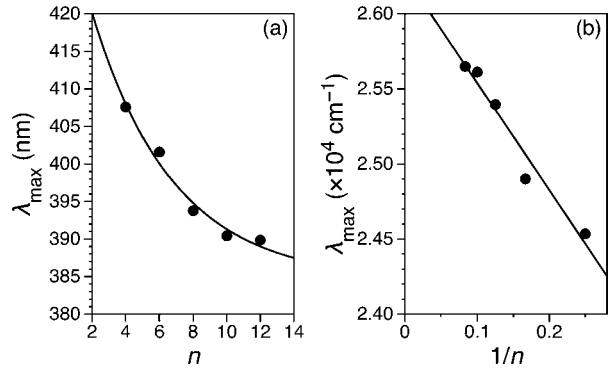

Figure 6. (a) Plot of the observed $\lambda_{max,FL}$ vs n; the solid line represents a fit to eq 1 ($\chi^2 = 5.13$). (b) Plot of $\lambda_{max,FL}$ vs $1/n$; the solid line represents a linear least-squares fit ($R^2 = 0.96$).

oP^{12}: $\Phi = 0.15$). As was the case for the UV/vis spectra, the oligomers exhibit essentially no solvatochromism in their fluorescence spectra (Figure S11), and the solid state spectrum of **oP^{12}** is essentially identical to that in solution (compare Figures 5 and S8).

Surprisingly, while there is a substantial bathochromic shift in the fluorescence when comparing **oP^2** to **oP^4**, the overall trend is a gradual *hypsochromic* shift in the fluorescence maximum as n increases, with simultaneous reduction of a shoulder at the long wavelength end of the spectrum. Although we do not believe that this is an electronic effect (see below), for the purpose of quantifying the magnitude of this shift it is interesting that the $\lambda_{max,FL}$ values also show a reasonable fit to eq 1 and a linear dependence on $1/n$ (Figure 6). The fit to eq 1 yields $\lambda_{\infty,FL} = 384 \pm 6$ nm, $\Delta\lambda_{FL} = -44 \pm 6$ nm, and $b_{FL} = 0.2 \pm 0.1$.

We were interested in further probing the nature of the two bands observed in the fluorescence spectra, hypothesizing, based on the NMR data, that they may arise from different emitting conformations. To this end, we acquired excitation spectra of **oP^4** as a function of emission wavelength, shown in Figure 7. Clearly, the excitation spectra are highly dependent on the monitored emission wavelength. Emission from the blue-shifted band in the fluorescence spectrum is preferentially excited by the extremes of short (ca. 240 nm) and long (300 nm) wavelengths, whereas emission from the red-shifted band is preferentially excited by intermediate (270 nm) wavelengths. These differences are also reflected in the emission spectra as a function of excitation wavelength (Figure S12). Similar, but less pronounced, behavior is observed for **oP^6**. The excitation spectra of **oP^2**, however, are independent of the monitored emission wavelength, as expected.

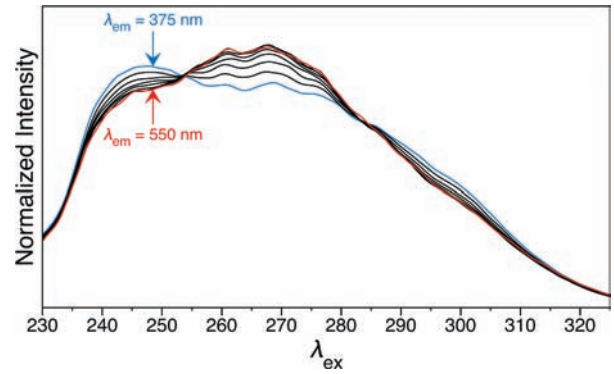

Figure 7. Excitation spectra of **oP^4** as a function of monitored emission wavelength (in dichloromethane). The extremes, 375 and 550 nm, are shown in blue and red, respectively. Intermediate emission wavelengths, in 25 nm increments, are shown in black. The spectra are normalized to the same total area. Note that in a 1.0 cm cuvette dichloromethane begins to absorb significantly for $\lambda < 245$ nm ($A = 0.05$).

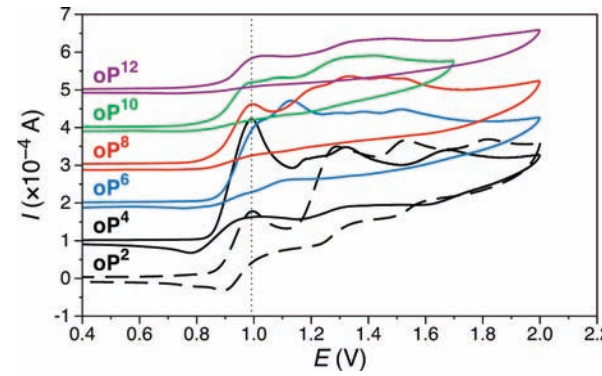

Figure 8. Cyclic voltammetry of **oP^n** vs $Ag/AgNO_3$ in anhydrous acetonitrile at a scan rate of 100 mV/s with tetra-*n*-butylammonium hexafluorophosphate as the supporting electrolyte. The dotted line is at $E = 0.99$ V. Each successive oligomer is offset by 1×10^{-4} A.

Electrochemistry. In order to probe differences in the abilities of the oligomers to delocalize charge, the **oP^n** series was studied by cyclic voltammetry as solutions in anhydrous acetonitrile with tetra-*n*-butylammonium hexafluorophosphate as the supporting electrolyte. As shown in Figure 8, the compounds **oP^4**–**oP^{12}** show clear oxidation peaks without corresponding reduction peaks on the return scan, suggesting that oxidation is chemically irreversible.[33] For all of the oligomers there is essentially no change in the position of the first oxidation peak as a function of n ($E_p \approx +0.99$ V vs $Ag/AgNO_3$), which occurs at the same potential as **oP^2**. Therefore, based on the cyclic voltammogram of **oP^2**, the entire **oP^n** series has oxidation potentials of $E_{ox} = 1.28$ V vs SCE.[34] Similarly, we estimate their HOMO levels at 5.6 eV.[35]

Discussion

Arguably, the defining feature of *o*-phenylenes compared to most other conjugated architectures is their inherently complex

(29) (a) *Electronic Materials: The Oligomer Approach*; Müllen, K., Wegner, G., Eds.; Wiley-VCH: Weinheim, 1998. (b) Martin, R. E.; Diederich, F. *Angew. Chem., Int. Ed.* **1999**, *38*, 1350–1377.
(30) Zhao, Y.; Campbell, K.; Tykwinski, R. R. *J. Org. Chem.* **2002**, *67*, 336–344.
(31) Meier, H.; Stalmach, U.; Kolshorn, H. *Acta Polym.* **1997**, *48*, 379–384.
(32) Eaton, D. F. *Pure Appl. Chem.* **1988**, *60*, 1107–1114.
(33) Repeat scans on the same solutions and experiments which stopped after the first oxidation (i.e., at 1.1 V) further indicated decomposition.

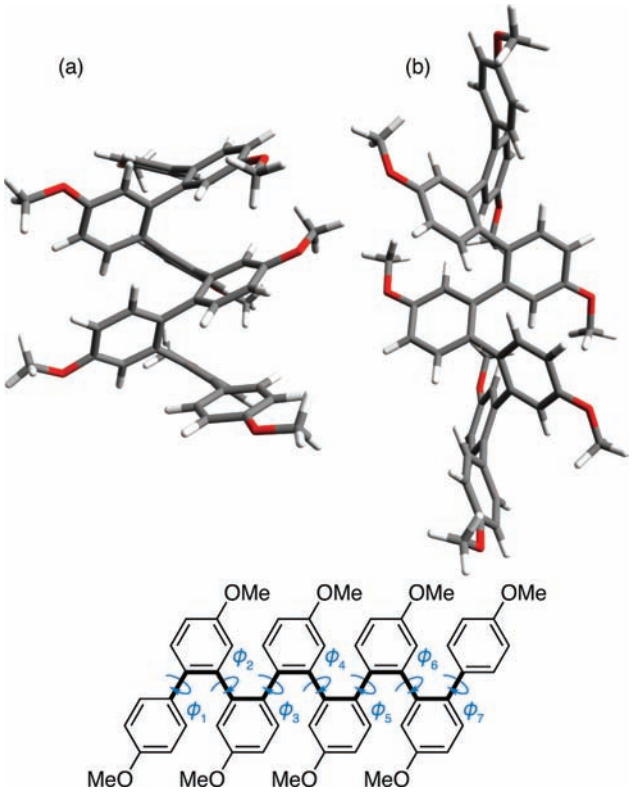

Figure 9. Limiting conformations of **oP^8** optimized at the B3LYP/6-31G(d) level. (a) "Closed" helix, with $\phi_2 = \phi_6 = 67°$, $\phi_3 = \phi_5 = 70°$, and $\phi_4 = 67°$ ($\phi_1 = \phi_7 = 46°$). (b) "Open" helix, with $\phi_2 = \phi_6 = -130°$, $\phi_3 = \phi_5 = -128°$, and $\phi_4 = -131°$ ($\phi_1 = \phi_7 = -133°$).

conformational behavior, due to various combinations of torsional angles along the internal biaryl bonds ϕ_2–ϕ_{n-2} (rotation about the terminal bonds ϕ_1 and ϕ_{n-1} is degenerate). Conformational analysis of the structurally related poly(2,3-quinoxaline)s has shown that, in an *o*-arylene polymer, these torsions can assume two stable limiting values (approximately 45° and 130° for the specific case of 2,3-quinoxalines).[36] Analysis of the **oP^n** series suggests that the behavior of these materials should be similar, as exemplified by the representative conformations of **oP^8** shown in Figure 9. In general, we have found that the internal biaryl bonds in the **oP^n** series can assume dihedrals of approximately ±70° or ±130°, based on minimizations at the B3LYP/6-31G(d) level (calculated using Gaussian 03[37]).

Although the various combinations of ϕ_i describe many possible conformations available to these structures, we begin by considering the two limiting cases. If all $\phi_i \approx 70°$, the conformation is best described as a tightly packed, stacked helical conformation that we refer to as the "closed" helix (Figure 9a). Alternatively, if all $\phi_i \approx 130°$, the oligomer is in an extended helical conformation we call the "open" helix (Figure 9b). The specific conformational state should have a substantial impact on the properties of an *o*-phenylene: the open helix should exhibit more effective orbital overlap since directly connected arenes are closer to coplanarity, whereas the closed helix should exhibit closer through-space contacts between arenes. In the case of Ito's poly(2,3-quinoxaline)s, most compounds studied were shown to favor the open helical conformation. Conversely, the solid-state structure of Simpkins' *o*-phenylene hexamer corresponds to the closed helix.

As discussed, the NMR characterization of the **oP^n** series suggests that interconversion between these various conformations is slow on the NMR time scale and that the overall pool is dominated by a 2-fold-symmetric (presumably C_2-symmetric) conformer. With this in mind, we turned our attention to the fluorescence spectra of **oP^4** (Figure 5). The distinct excitation spectra for the two bands suggest that they arise from different emitting species. Since **oP^4** itself has only one internal biaryl bond (ϕ_2, see Figure 5), we believe that these two bands likely represent emission from the two distinct conformational states (i.e., $\phi_2 \approx \pm 70°$ vs $\pm 130°$). It follows, since the red-shifted emission band decreases in relative intensity as *n* increases, that one particular torsional state becomes more prevalent for the longer oligomers. This assertion is reasonable if one assumes that the two biaryl bonds near the ends of the oligomers (e.g., ϕ_2 and ϕ_6 in Figure 9) behave differently from those closer to the center (e.g., ϕ_3, ϕ_4, and ϕ_5). Obviously, as the oligomer is lengthened, it is only the number of central biaryl bonds that increases.

Our hypothesis is that, in solution, the internal biaryl torsion angles (ϕ_3–ϕ_5 for **oP^8**) are biased toward the ±70° states and that the external dihedrals (ϕ_2/ϕ_6) are more conformationally mobile, in that they are also able to sample the ±130° states. In other words, we believe that the closed helix is a better representation of the overall conformation of these structures, with some conformational disorder at the ends. This hypothesis is supported by several pieces of indirect evidence.

First, analogues of the closed helical conformation are favored in all similar structures in the literature of which we are aware. The most significant of these is the solid-state structure of the *o*-phenylene hexamer reported by Simpkins and solution-phase analysis (ROESY NMR) of a related *o*-phenylene tetramer.[25] Similar conformations have also been reported for the structurally similar oligo(β-pyrrole)s[38] and oligo(2,3-thiophene)s.[39] The key exceptions to this behavior are Ito's poly(2,3-quinoxaline)s, but these architectures are typically functionalized with bulky substituents that would favor the open helical conformation due to sterics. Moreover, the 2,3-quinoxaline backbone, which lacks hydrogen atoms *ortho* to the biaryl bonds, should be predisposed toward the more planar open helical conformation (i.e., just as 2-phenylpyrimidine is planar in the ground state, whereas biphenyl is twisted[40]). It is noteworthy that the Ito group has reported the crystal structure of an oligo(2,3-naphthalene) tetramer that lacks bulky substituents and does possess the *ortho* hydrogen atoms; in contrast to their other reported structures, it does indeed appear to adopt a closed helical conformation in the solid state.[41]

Second, the solid-state structures of **oP^4** and **oP^6** (Figure 2) suggest that the ±70° state is favored for the internal bonds.

(34) Determined as the average of the anodic and cathodic peak potentials, referenced to ferrocene ($E_{ox} = 0.450$ vs SCE).
(35) Estimated from the onsets of the oxidation peak relative to ferrocene as a standard, $E_{HOMO} = -(E'_{oP^n} - E'_{Fc}) + 4.8$ eV.
(36) Ito, Y.; Ihara, E.; Murakami, M.; Sisido, M. *Macromolecules* **1992**, *25*, 6810–6813.
(37) Frisch, M. J.; et al. *Gaussian 03*, revision D.02; Gaussian, Inc.: Wallingford, CT, 2004.
(38) Magnus, P.; Danikiewicz, W.; Katoh, T.; Huffman, J. C.; Folting, K. *J. Am. Chem. Soc.* **1990**, *112*, 2465–2468.
(39) (a) Marsella, M. J.; Yoon, K.; Almutairi, A.; Butt, S. K.; Tham, F. S. *J. Am. Chem. Soc.* **2003**, *125*, 13928–13929. (b) Almutairi, A.; Tham, F. S.; Marsella, M. J. *Tetrahedron* **2004**, *60*, 7187–7190.
(40) Barone, V.; Commisso, L.; Lelj, F.; Russo, N. *Tetrahedron* **1985**, *41*, 1915–1918.
(41) Motomura, T.; Nakamura, H.; Suginome, M.; Murakami, M.; Ito, Y. *Bull. Chem. Soc. Jpn.* **2005**, *78*, 142–146.

oP^4 adopts the closed helical conformation. **oP^6** does not; however, it is the ends of the oligomer ($\phi_2 \approx \phi_4 \approx 137°$) that deviate from the closed helical state, and not the internal bond ($\phi_3 \approx 74°$). For convenience, we define this type of conformation, a closed helix except that the monomers at the ends of the oligomer are flipped away from the helical path, as a "quasi-closed" helix. We were, unfortunately, unable to obtain crystal structures of the longer oligomers; however, conformational energy searches at the MMFF level (which give high-quality geometries for the related oligo(2,3-thiophene)s[39a]) invariably identify the closed helical conformation as the most stable 2-fold-symmetric conformer for each of **oP^4**−**oP^{12}**.[42] Unfortunately, gas-phase B3LYP/6-31G(d) calculations (described below) do not provide clear guidance as to the relative stability of the conformers, as all optimized geometries were found to be very close energetically (e.g., $\Delta E < 1.1$ kcal/mol for all considered conformations of **oP^6**).

Third, the emission and excitation spectra support the prevalence of the closed helical conformers. The open helix would be expected to exhibit stronger through-bond conjugation simply because the arene subunits are closer to coplanarity (twists of ca. 50° vs 75° for the open and closed helices, respectively). For **oP^4**, the longer wavelength emission does indeed correspond to the longer wavelength excitation maximum, suggesting that it arises from the open conformer. This assignment of the excitation spectra is qualitatively supported by TD-DFT calculations of the two **oP^4** conformers at the PCM-TD-PBE0/6-311+G(2d,p)//B3LYP/6-31G(d) level (Figure S13).[43] The calculations confirm that the most intense transitions for the open helical conformer should be red-shifted compared to the closed helix. Further, the predicted UV/vis transitions for the closed helix do include a weak but significant long-wavelength transition, which is consistent with the shoulder in the excitation spectra. These theoretical results do not predict that this weak low-energy transition for the closed helix will be red-shifted relative to the open helix, but we note that the difference between these transitions is well within the expected error for these calculations (ca. 0.1 eV, which is 7 nm at 300 nm)[43] and also consistent with the known tendency of TD-DFT calculations to overestimate the extent of conjugation in oligomeric π-systems.[44]

On the basis of the hypothesis that the **oP^n** oligomers can be broadly described by the closed helix model, we carried out geometry minimizations (B3LYP/6-31G(d)) of this conformer for each member of the series, shown in Figure 10. For comparison, we also carried out similar calculations for the open helix and the quasi-closed helix conformers, with their structures and frontier orbitals shown in Figures S14 and S15. It must be noted that, while there are very obvious and significant differences between the calculated electronic structures of the fully open and fully closed helices, the quasi-closed and fully closed helices are functionally equivalent in the sense that they provide identical qualitative interpretations of the experimental data.

Strikingly, the calculated HOMOs of the **oP^n** oligomers are localized at their ends, presumably because of improved orbital overlap between the terminal monomers (e.g., for **oP^{12}**, $\phi_1 = \phi_{11} = 46°$, whereas the mean interior ϕ_i is 69°). This consequence of the geometry of the *o*-phenylene backbone is very unusual, as the frontier orbitals of unfunctionalized conjugated oligomers are typically located near their centers.[4d,45] The LUMOs, conversely, are localized in the interiors of the oligomers. In the case of **oP^{12}**, the LUMO spans essentially the second through fifth monomers (from either end) with significantly less density at the direct center. Interestingly, close examination of the calculated LUMOs does suggest some through-space overlap between the stacked arenes.

This picture of the electronic structure of the **oP^n** series can be used to rationalize some of their unusual properties. For example, by cyclic voltammetry, we had observed that there was no substantial change in the first oxidation potential over the entire series, implying that there is little change in HOMO energies (5.6 eV) as the oligomers are lengthened. From the DFT calculations, it is now clear why this is the case: for all oligomers, the HOMOs are delocalized over just two units at the termini, and these subunits are directly analogous to **oP^2**. Interestingly, the actual oxidation potentials ($E_{ox} = 1.28$ V vs SCE) are quite similar to that of an infinite unsubstituted *p*-phenylene polymer (ca. 1.3 V vs SCE),[4d] which can be rationalized by assuming that the electron-donating methoxy groups compensate for the reduced conjugation. The calculated HOMO levels are similar to those of polyphenylenes in general (5.8−6.0 eV)[46] and are comparable to other classes of structurally related conjugated polymers, such as dialkoxy-substituted poly(*p*-phenylene ethynylene)s (5.8 eV)[47] and polyfluorenes (5.65 eV).[48]

One of the most surprising findings of our study is the observation that changes in the UV/vis spectra of the **oP^n** series are observed even at large *n*. Comparison of the overall effect of conjugation determined for the **oP^n** series, $\Delta\lambda_{UV} = 39 \pm 2$ nm, with those determined for other conjugated oligomers suggests that it is modest and roughly comparable to some *p*-phenylene ethynylenes ($\Delta\lambda_{UV} \approx 40$ nm),[49] although in general it is a factor of 2 or 3 lower than most related conjugated systems (e.g., $\Delta\lambda_{UV} = 100-140$ nm for *p*-phenylenes, *p*-phenylene vinylenes, or other *p*-phenylene ethynylenes).[31,50] Conversely, the *extent* of conjugation, $b = 0.52 \pm 0.05$, implies that the delocalization spans a remarkably long range ($b = 0.5-0.7$ for *p*-phenylenes, ca. 0.5 for phenylene vinylenes, 1.0 for phenylene ethynylenes). This gives rise to the surprisingly long effective conjugation length of $n_{ecl} \approx 8$. This value is quite similar to that for alkoxy-substituted *p*-phenylenes with relatively large torsional angles between the repeat units (53°),[51] for which n_{ecl}

(42) These calculations consider all possible 2-fold permutations of the biaryl torsions. For **oP^4**−**oP^{10}**, the closed helix is identified as the most stable conformer. For **oP^{12}** it is the most stable 2-fold-symmetric conformer (i.e., consistent with the major conformer identified by NMR).

(43) Jacquemin, D.; Perpète, E. A.; Ciofini, I.; Adamo, C. *Acc. Chem. Res.* **2009**, *42*, 326–334.
(44) Gierschner, J.; Cornil, J.; Egelhaaf, H.-J. *Adv. Mater.* **2007**, *19*, 173–191.
(45) (a) Bruschi, M.; Giuffreda, M. G.; Lüthi, H. P. *ChemPhysChem* **2005**, *6*, 511–519. (b) Yang, L.; Ren, A.-M.; Feng, J.-K.; Wang, J.-F. *J. Org. Chem.* **2005**, *70*, 3009–3020. (c) Ran, X.-Q.; Feng, J.-K.; Liu, Y.-L.; Ren, A.-M.; Zou, L.-Y.; Sun, C.-C. *J. Phys. Chem. A* **2008**, *112*, 10904–10911. (d) Lukeš, V.; Aquino, A. J. A.; Lischka, H.; Kauffmann, H.-F. *J. Phys. Chem. B* **2007**, *111*, 7954–7962.
(46) Grimsdale, A. C.; Müllen, K. *Adv. Polym. Sci.* **2008**, *212*, 1–48.
(47) Montali, A.; Smith, P.; Weder, C. *Synth. Met.* **1998**, *97*, 123–126.
(48) Beaupré, S.; Leclerc, M. *Macromolecules* **2003**, *36*, 8986–8991.
(49) Schumm, J. S.; Pearson, D. L.; Tour, J. M. *Angew. Chem., Int. Ed. Engl.* **1994**, *33*, 1360–1363.
(50) Ickenroth, D.; Weissmawnn, S.; Rumpf, N.; Meier, H. *Eur. J. Org. Chem.* **2002**, 2808–2814.
(51) Based on optimization at the B3LYP/6-31G(d) level.

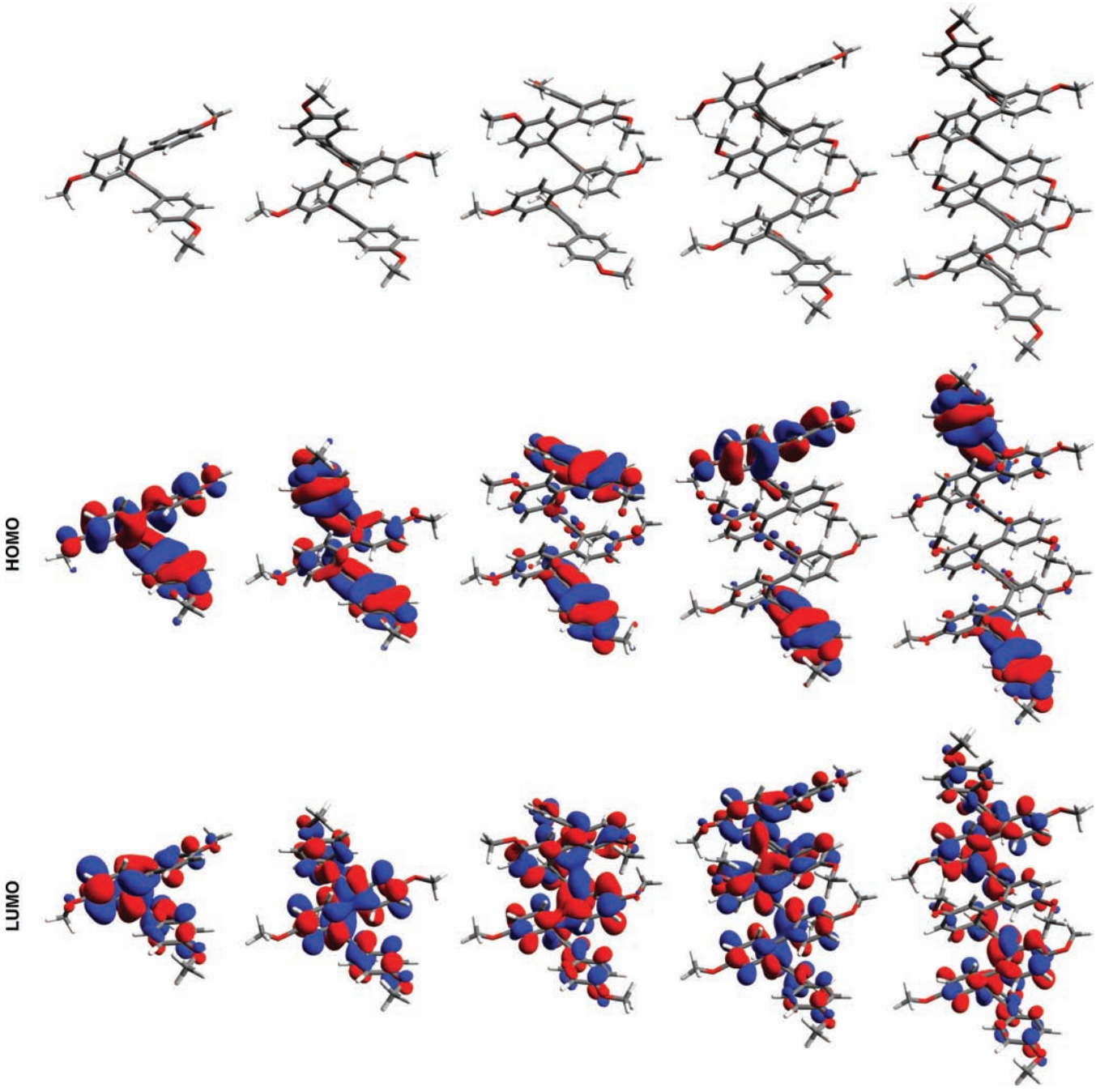

Figure 10. Calculated B3LYP/6-31G(d) geometries (top), HOMOs (middle), and LUMOs (bottom) for the closed helical conformations. The orbitals are displayed with isosurface values of 0.02.

≈ 9,[52] although it is significantly lower than that for ladder *p*-phenylenes with enforced planarity between the rings, for which $n_{ecl} \geq 12$.[46,53,54] The experimental effective conjugation length is in good agreement with the extent of the calculated LUMO levels, which appear to be delocalized over at most five consecutive arenes, and thus would be expected to be unaffected beyond $n \approx 10$.

The unusual conformational behavior of these oligomers can be used to rationalize their UV/vis behavior compared to most other conjugated systems. Significant conjugative effects are observed over a relatively large number of arene units, which we ascribe to the rigidity of the *o*-phenylene architecture. Conversely, because of the considerable twisting of the *o*-phenylene backbone, the overall effect of conjugation ($\Delta\lambda$) is small, although it is surprisingly large considering that previous discussion in the literature had suggested that delocalization in an *o*-phenylene should extend over only biphenyl-like subunits.[7a] As a consequence of this modest $\Delta\lambda$, the UV/vis spectra of the **oP^n** series are in general blue-shifted by ca. 50 nm compared to *p*-phenylenes of similar lengths (both unsubstituted and

(52) (a) Remmers, M.; Müller, B.; Martin, K.; Räder, H.-J.; Köhler, W. *Macromolecules* **1999**, *32*, 1073–1079. (b) Grimsdale, A. C.; Müllen, K. *Adv. Polym. Sci.* **2006**, *199*, 1–82.

(53) Grimme, J.; Kreyenschmidt, M.; Uckert, F.; Müllen, K.; Scherf, U. *Adv. Mater.* **1995**, *7*, 292–295.

(54) The n_{ecl} values quoted here differ slightly from the literature reports, as we have reanalyzed the data with eqs 1 and 2 for consistency.

alkoxy-substituted).[4d,52a] We are currently investigating how this weak but long-range conjugation will affect the wire-like behavior of these systems.

The fluorescence spectra for **oP^4**−**oP^{12}** undergo a blue shift with increasing length; consequently, while the emission of **oP^4** is actually red-shifted relative to *p*-phenylene tetramers, extrapolation suggests that an **oP^n** polymer should exhibit blue-shifted emission compared to poly(*p*-phenylene)s.[4d,52a] This unusual hypsochromic shift with increasing *n* is almost certainly not due to an electronic effect, since it is not mirrored in the UV/vis spectra (and would appear to violate the basic principles of a simple particle-in-a-box model). It has been shown that certain donor−acceptor-substituted conjugated oligomers exhibit hypsochromic shifts with increasing length due to attenuation of intramolecular charge-transfer interactions.[55] There is, however, no suggestion of significant charge transfer in the excited states of the **oP^n** series, given the lack of solvatochromism in the fluorescence spectra. Instead, we believe that the observed hypsochromic shift is likely due to varying abilities of the oligomers to undergo geometric changes in the excited state. It is well-known that *p*-phenylenes undergo planarization in the excited state, leading to large Stokes shifts.[56] Planarization should obviously not be possible for the much more sterically encumbered *o*-phenylenes, where, for closed helices, it essentially corresponds to compression of the spring-like conformers. We suspect, however, that the longer **oP^n** oligomers will be less able to accommodate these geometric changes since they would have to occur within their sterically less-forgiving interiors. In essence, the longer oligomers appear to undergo lessened geometric rearrangements in their excited states, leading to reduced Stokes shifts. Alternatively, it may be that the blue shift of the fluorescence maxima simply reflects the changing conformational pool as *n* increases (i.e., decrease of ϕ_i subunits in the 70° state). Additional experiments to more accurately assess the conformational behavior and careful theoretical studies of excited state geometries will be required to fully understand this phenomenon.

(55) (a) Meier, H. *Angew. Chem., Int. Ed.* **2005**, *44*, 2482–2506. (b) Meier, H.; Gerold, J.; Kolshorn, H.; Mühling, B. *Chem.—Eur. J.* **2004**, *10*, 360–370.

(56) (a) Momicchioli, F.; Bruni, M. C.; Baraldi, I. *J. Phys. Chem.* **1972**, *76*, 3983–3990. (b) Heimel, G.; Daghofer, M.; Gierschner, J.; List, E. J. W.; Grimsdale, A. C.; Müllen, K.; Beljonne, D.; Brédas, J.-L.; Zojer, E. *J. Chem. Phys.* **2005**, *122*, 054501.

Conclusions

We have developed an iterative synthetic approach to *o*-phenylene oligomers, which has allowed the synthesis of a homologous series of these compounds up to the dodecamer. Evaluation of their absorption, emission, and electrochemical properties as a function of oligomer length reveals very unusual behavior, including the following: (1) significant bathochromic shifts to the UV/vis spectra, suggesting that conjugation extends much farther along the *o*-phenylene backbone than previously thought; (2) significant hypsochromic shifts to the fluorescence spectra; and (3) oxidation potentials (and HOMO energies) that are largely independent of length. These unusual properties appear to result from the conformational behavior of the oligomers, which is more complex than that of typical conjugated materials. We are currently exploring methods to probe this conformational behavior directly and the use of the *o*-phenylene motif as a means to organize other chromophores.

Acknowledgment. C.S.H., J.H., and J.L.C. acknowledge support by the National Science Foundation (CHE-0910477), Miami University, and the donors of the American Chemical Society Petroleum Research Fund (47926-G7). R.R., S.H.W., and K.T. acknowledge support from the National Science Foundation (Chemistry). L.D. and S.Z. acknowledge support from the National Science Foundation (CHM-0616436).

Supporting Information Available: NMR spectra of **oP^n**, GPC traces, UV/vis spectra in methanol and cyclohexane, solid-state UV/vis and fluorescence spectra of **oP^{12}**, normalized UV/vis spectra and hypochromicity, extrapolations used for UV/vis λ_{ext} values, fluorescence spectra in methanol and cyclohexane, emission spectra of **oP^4** as a function of excitation wavelength, calculated oscillator strengths of **oP^4**, calculated geometries and FMOs for open helical conformers, calculated geometries and FMOs for quasi-closed helical conformers, full experimental procedures, and complete ref 37. This material is available free of charge via the Internet at http://pubs.acs.org.

JA106050S